IEEE Access
Multidisciplinary : Rapid Review : Open Access Journal

Received 30 April 2023, accepted 18 May 2023, date of publication 29 May 2023, date of current version 8 June 2023.
Digital Object Identifier 10.1109/ACCESS.2023.3280543

RESEARCH ARTICLE

Extended Discrete-Time Quasi-Sliding Mode Control for VTOL UAV in the Presence of Uncertain Disturbances

IMIL HAMDA IMRAN[1], AZHAR M. MEMON[1], DILEK FUNDA KURTULUS[2], SRIKANTH GOLI[1], AND LUAI MUHAMMAD ALHEMS[1]
[1]Applied Research Center for Metrology, Standards, and Testing, King Fahd University of Petroleum and Minerals, Dhahran 31261, Saudi Arabia
[2]Department of Aerospace Engineering, Middle East Technical University, 06800 Ankara, Turkey

Corresponding author: Imil Hamda Imran (imil.imran@kfupm.edu.sa)

ABSTRACT The discrete control problem of vertical take-off and landing unmanned aerial vehicle (VTOL UAV) in the presence of time-varying uncertain disturbances is developed in this paper. The complexity of control problem is managed by dividing the dynamical model into two subsystems i.e. translational dynamics and rotational dynamics, where each subsystem is composed of three states. A discrete-time quasi-sliding mode control (DTQSMC) is extended to maintain the trajectory tracking control by proposing a new-reaching law for VTOL UAV. A robust controller is designed to handle unknown time-varying disturbances acting upon the translational and rotational dynamics. Moreover, the proposed controller is designed to reduce the chattering issue that commonly appears in conventional sliding mode control (SMC). Rigorous mathematical proof is presented to analyze the stability of the entire closed-loop system. The performance of this design is demonstrated with numerous numerical analyses and simulations.

INDEX TERMS Chattering, discrete-time, disturbances, quasi-sliding mode control, time-varying, UAV, VTOL.

I. INTRODUCTION

Research and development on VTOL UAVs have attracted the attention of numerous researchers and industries in recent decades. UAV deployment has many potential benefits as compared to conventional methods operated by a human. Moreover, VTOL UAV deployment can also increase efficiency by saving time and cost. UAV with VTOL configuration has some advantages such as a simple transition mechanism and ease to take off and land in a narrow area. It can be used in various applications of UAVs such as data collection, monitoring, mapping, geographical photography, inspection, surveillance, search and rescue, forest-fire detection, creative industries, and various civil applications [9], [14], [28]. From the control engineer's view, one of the trendiest research problems is to develop an autonomous operation of UAVs that can maintain the VTOL settings with less dependent on the human operator. Many control strategies have been studied for UAVs under various scenarios. One of the most challenging parts of realistic situations is to design control schemes with nonlinear dynamics and the presence of external disturbances.

VTOL UAV is an under-actuated nonlinear system, with four control inputs to handle a highly coupled six output states. It is composed of three states related to translational dynamics allowing UAV to move in backward, forward, lateral, and vertical directions. The remaining states are related to rotational dynamics referred to as roll, pitch, and yaw angles. The main focus of the trajectory tracking problem with the VTOL mission is to design the control scheme for both translational and rotational dynamics in the presence of disturbances. The nonlinear control approach plays an important role in maintaining UAV motion with complete nonlinear behavior. Several research problems have been investigated to tackle the trajectory tracking problem. One of the common methods is the feedback linearization method as developed in [34] and [40] for non-VTOL configurations.

The associate editor coordinating the review of this manuscript and approving it for publication was Mohammad Alshabi.

In fact, uncertain external disturbances may act on the system dynamics in numerous practical situations. These uncertainties may cause more complex technical challenges in designing controllers. Hence, the feedback linearization approach cannot be simplified and extended to handle this issue. In general, there are two main directions to tackle the uncertainties in the closed-loop systems [21]. The first is to use adaptive control scheme. The idea behind this method is to estimate and cancel the uncertainties in the system dynamics. In this way, the controller guarantees to handle the uncertainties by proposing adaptive law in the feedback controller.

Model reference adaptive control (MRAC) is one of the popular adaptive schemes to deal with uncertainties. By using the certainty equivalence principle, adaptive law, and reference model are added to the feedback control design to estimate the unknown constant parameters [30]. This technique has a major drawback to guarantee stability as investigated in [2]. The L_1 adaptive control was developed by adding a linear filter in the control structure to handle this problem [17]. Some interesting results in adaptive control using Immersion and invariance (I&I) were studied to handle unknown constant parameters [3], [25]. However, most of the adaptive schemes are to handle the unknown constant parameters [6]. As a result, the use of adaptive control approaches in general cannot handle time-varying disturbances. Some results have been presented for time-varying disturbances in limited cases [5], [20], [22], [36].

Another method proposed in the literature to handle uncertainties is model predictive control (MPC). For example, adaptive MPC was developed with extended state observer (ESO) for UAVs under a networked setting [39]. Another common technique used to handle the uncertainties is intelligent computation which can be categorized in the adaptive control line. For example, neural networks (NNs) were developed for multi-agent systems [7], [8] and genetic algorithm (GA) for a robotic manipulator [27]. However, this approach has one crucial issue in handling uncertainties, where this method requires a high-performance embedded computer in many cases. In other words, it can only be implemented in limited practical situations.

The second major research direction is robust control. The idea behind this controller is to guarantee stability by dominating the uncertainties within a certain bound. Compared with adaptive control approach, it is more flexible to be implemented for systems with time-varying uncertainties. SMC is one of the most popular methods in this direction. This approach is widely implemented in many practical settings in the continuous-time domain by forcing the states to follow desired sliding surface [19], [24]. SMC was developed to handle uncertainties in the discrete-time domain in [32]. However, this technique has chattering problems due to the presence of a signum function in the control structure. Discrete-time robust MRAC using SMC and adaptive super-twisting MRAC for first-order systems with chattering attenuation were compared in [16].

Control problem for an under-actuated UAV with a VTOL mission becomes more complicated. An early study introduced a control scheme for a micro VTOL UAV without disturbance [4]. More complex control problems in the presence of disturbances were studied by proposing disturbance observer-based control method in [26], higher-order-observer-based dynamic SMC [29] and adaptive SMC in [1], [23]. An integrated disturbance observer, MPC, and sliding mode nonlinear inverse were proposed for a tail rotor tilting three ducted fans VTOL-UAV [18].

Some interesting robust control methods were developed for fault tolerance control (FTC) of VTOL UAV in the continuous-time domain. For example, an adaptive SMC for FTC of VTOL UAV was designed in [15] and [35] to handle uncertainties and faults. In [37], a robust passive FTC was proposed for tracking control of VTOL UAV with partial propeller fault and external disturbance. The more advanced result was presented using adaptive SMC for multi-UAVs subject to an aerodynamic disturbance in [1].

In the practical setting, the control systems of UAVs rely on sensor and actuator measurements. These measurements are used by the controller to generate a new control input for the dynamical model in a particular sampling time. From the above literature, all controller schemes were designed in the continuous-time domain. It means that the controllers were not presented the practical situations. A result using conventional sliding mode control for the non-VTOL mission with chattering issue was investigated without disturbance in the discrete-time domain [38].

In this paper, a control scheme is developed for an under-actuated nonlinear VTOL UAV with uncertainties. The control scheme is designed in the discrete-time domain to represent the real application setting whereby the time-continuous plant is controlled by a discrete-time controller embedded in a microprocessor. Inspired by [12], a reaching law is proposed for VTOL UAV to guarantee the convergence of sliding surfaces to zero equilibrium points. The tracking control stability is guaranteed by adding robust terms to the control structure to handle time-varying uncertain external disturbances added in both translational and rotational dynamics. This extension is very important to tackle the control problem to deal with uncertainties and nonlinear dynamics in the discrete-time domain. Moreover, the potential benefits of UAV deployment can be expanded by designing a controller with VTOL configuration, particularly for UAV operating in confined spaces such as near walls and narrow areas.

The remainder of this paper is organized as follows. The dynamical model of VTOL UAV is presented in Section II. Following that, the proposed tracking control design with its stability analysis for both the outer and inner loop of VTOL UAV is presented in Section III. Then in Section IV, the performance of the proposed design is demonstrated by conducting numerous numerical analyses and simulation results. The summary of this paper and a brief suggestion for future research direction are presented in Section V.

II. SYSTEM DYNAMICS OF VTOL UAV

Consider the general motion of VTOL UAV expressed by the following states

$$\eta_1 = \begin{bmatrix} x \\ y \\ z \end{bmatrix}, \quad \eta_2 = \begin{bmatrix} \phi \\ \theta \\ \psi \end{bmatrix},$$

where η_1 is a position vector consisting of forward (x), lateral (y) and vertical (z) states and η_2 is an orientation vector consisting of roll (ϕ), pitch (θ) and yaw (ψ) states. Figure 1 illustrates the coordinate frames of η_1 and η_2.

The translational and rotational dynamics of VTOL UAV with the presence of disturbance in the continuous-time domain are represented by the following state space [4], [23]

$$\ddot{x}(t) = (\cos\phi(t)\sin\theta(t)\cos\psi(t) + \sin\phi(t)\sin\psi(t)) \times \frac{u_t(t)}{m} \tag{1}$$

$$\ddot{y}(t) = (\cos\phi(t)\sin\theta(t)\sin\psi(t) - \sin\phi(t)\cos\psi(t)) \times \frac{u_t(t)}{m} \tag{2}$$

$$\ddot{z}(t) = -g + \delta_z(t) + (\cos\phi(t)\cos\theta(t))\frac{u_t(t)}{m} \tag{3}$$

$$\ddot{\phi}(t) = w_\phi f_\phi(t) + \delta_\phi(t) + \frac{\tau_\phi(t)}{I_x} \tag{4}$$

$$\ddot{\theta}(t) = w_\theta f_\theta(t) + \delta_\theta(t) + \frac{\tau_\theta(t)}{I_y} \tag{5}$$

$$\ddot{\psi}(t) = w_\psi f_\psi(t) + \delta_\psi(t) + \frac{\tau_\psi(t)}{I_z}, \tag{6}$$

where

$$w_\phi = \frac{I_y - I_z}{I_x}, \quad f_\phi(t) = \dot{\theta}(t)\dot{\psi}(t)$$
$$w_\theta = \frac{I_z - I_x}{I_y}, \quad f_\theta(t) = \dot{\phi}(t)\dot{\psi}(t)$$
$$w_\psi = \frac{I_x - I_y}{I_z}, \quad f_\psi(t) = \dot{\phi}(t)\dot{\theta}(t).$$

The mass of VTOL UAV is denoted by m and gravitational acceleration is denoted by g. The inertia parameters with respect to x, y, and z axes are represented by I_x, I_y, and I_z, respectively. The total force is denoted by u_t and the torques acting on the body frame in roll, pitch, and yaw directions are denoted by τ_ϕ, τ_θ, and τ_ψ, respectively. Note that Both ϕ and θ angles are constrained between $-\frac{\pi}{2}$ to $\frac{\pi}{2}$ i.e. $\cos\phi$ and $\cos\theta$ are non-zero.

The external disturbances are represented by $\delta_z(t)$, $\delta_\phi(t)$, $\delta_\theta(t)$, and $\delta_\psi(t)$ satisfying the following assumption.

Assumption 1: The external disturbances acting on translational and rotational dynamics of VTOL UAV have boundaries such that $|\delta_z(t)| \leq d_z$, $\left|\delta_\phi(t)\right| \leq d_\phi$, $|\delta_\theta(t)| \leq d_\theta$ and $\left|\delta_\psi(t)\right| \leq d_\psi$ where d_z, d_ϕ, d_θ, and d_ψ are some constants. Note that all $\delta_z(t)$, $\delta_\phi(t)$, $\delta_\theta(t)$, and $\delta_\psi(t)$ are unknown. Only d_z, d_ϕ, d_θ, and d_ψ are available for feedback control design.

FIGURE 1. Earth and body-fixed reference frame of VTOL UAV.

The dynamical model of VTOL UAV in the discrete-time domain is formulated from the continuous-time model using the following forward Euler method

$$\dot{x}(k) = \frac{x(k+1) - x(k)}{t_s}$$
$$\dot{y}(k) = \frac{y(k+1) - y(k)}{t_s}$$
$$\dot{z}(k) = \frac{z(k+1) - z(k)}{t_s}$$
$$\dot{\phi}(k) = \frac{\phi(k+1) - \phi(k)}{t_s}$$
$$\dot{\theta}(k) = \frac{\theta(k+1) - \theta(k)}{t_s}$$
$$\dot{\psi}(k) = \frac{\psi(k+1) - \psi(k)}{t_s},$$

where k and $k+1$ are the time step at k and $k+1$ with time sampling t_s, respectively. It is obvious to see that

$$x(k+1) = x(k) + t_s\dot{x}(k) \tag{7}$$
$$y(k+1) = y(k) + t_s\dot{y}(k) \tag{8}$$
$$z(k+1) = z(k) + t_s\dot{z}(k) \tag{9}$$
$$\phi(k+1) = \phi(k) + t_s\dot{\phi}(k) \tag{10}$$
$$\theta(k+1) = \theta(k) + t_s\dot{\theta}(k) \tag{11}$$
$$\phi(k+1) = \phi(k) + t_s\dot{\phi}(k). \tag{12}$$

By using a similar argument, the following can be generated

$$\dot{x}(k+1) = \dot{x}(k) + t_s\ddot{x}(k) \tag{13}$$
$$\dot{y}(k+1) = \dot{y}(k) + t_s\ddot{y}(k) \tag{14}$$
$$\dot{z}(k+1) = \dot{z}(k) + t_s\ddot{z}(k) \tag{15}$$
$$\dot{\phi}(k+1) = \dot{\phi}(k) + t_s\ddot{\phi}(k) \tag{16}$$
$$\dot{\theta}(k+1) = \dot{\theta}(k) + t_s\ddot{\theta}(k) \tag{17}$$
$$\dot{\phi}(k+1) = \dot{\phi}(k) + t_s\ddot{\phi}(k). \tag{18}$$

By substituting (13-18) to (1-6), the dynamical model of VTOL UAV can be generated in the discrete-time domain as represented by

$$x(k+1) = x(k) + t_s\dot{x}(k)$$

$$\dot{x}(k+1) = \dot{x}(k) + t_s\Big(\cos\phi(k)\sin\theta(k)\cos\psi(k) + \sin\phi(k)\sin\psi(k)\frac{u_t(k)}{m}\Big) \tag{19}$$

$$y(k+1) = y(k) + t_s\dot{y}(k)$$
$$\dot{y}(k+1) = \dot{y}(k) + t_s\Big(\cos\phi(k)\sin\theta(k)\sin\psi(k) - \sin\phi(k)\cos\psi(k)\frac{u_t(k)}{m}\Big) \tag{20}$$

$$z(k+1) = z(k) + t_s\dot{z}(k)$$
$$\dot{z}(k+1) = \dot{z}(k) + t_s\Big(-g + \delta_z(k) + (\cos\phi(k)\cos\theta(k))\frac{u_t(k)}{m}\Big) \tag{21}$$

$$\phi(k+1) = \phi(k) + t_s\dot{\phi}(k)$$
$$\dot{\phi}(k+1) = \dot{\phi}(k) + t_s\Big(w_\phi f_\phi(k) + \delta_\phi(k) + \frac{\tau_\phi(k)}{I_x}\Big) \tag{22}$$

$$\theta(k+1) = \theta(k) + t_s\dot{\theta}(k)$$
$$\dot{\theta}(k+1) = \dot{\theta}(k) + t_s\Big(w_\theta f_\theta(k) + \delta_\theta(k) + \frac{\tau_\theta(k)}{I_y}\Big) \tag{23}$$

$$\psi(k+1) = \psi(k) + t_s\dot{\psi}(k)$$
$$\dot{\psi}(k+1) = \dot{\psi}(k) + t_s\Big(w_\psi f_\psi(k) + \delta_\psi(k) + \frac{\tau_\psi(k)}{I_z}\Big), \tag{24}$$

where

$$f_\phi(k) = \dot{\theta}(k)\dot{\psi}(k)$$
$$f_\theta(k) = \dot{\phi}(k)\dot{\psi}(k)$$
$$f_\psi(k) = \dot{\phi}(k)\dot{\theta}(k).$$

III. PROPOSED CONTROL DESIGN

In this section, a discrete robust control scheme is designed for VTOL UAV under uncertain disturbances. Let the desired trajectory of x, y, z, ϕ, θ and ψ are denoted by x_d, y_d, z_d, ϕ_d, θ_d and ψ_d, respectively. The main objective of the proposed controller is to guarantee all states of VTOL UAV to follow the desired trajectories.

A. TRANSLATIONAL CONTROL DESIGN

VTOL UAV is an under-actuated system where the number of control inputs is less than the number of states, where $x(k)$ and $y(k)$ positions cannot be controlled directly using $u_t(k)$. The $\phi_d(k)$ and $\theta_d(k)$ state variables are generated using error position and velocity of $x(k)$ and $y(k)$ as represented by

$$\phi_d(k) = \lambda_{y_1}(y(k) - y_d(k)) + \lambda_{y_2}(\dot{y}(k) - \dot{y}_d(k)) \tag{25}$$
$$\theta_d(k) = -\lambda_{x_1}(x(k) - x_d(k)) - \lambda_{x_2}(\dot{x}(k) - \dot{x}_d(k)), \tag{26}$$

where $\lambda_{x_1}, \lambda_{x_2}, \lambda_{y_1}$, and λ_{y_2} are some positive constants.

There exists an external disturbance $\delta_z(k)$ in the dynamical model (21). As a result, full feedback linearization method cannot be applied to handle the uncertainties. To design a robust controller, the error of z position is defined to be

$$e_z(k) = z(k) - z_d(k). \tag{27}$$

It is obvious to see that

$$\dot{e}_z(k) = \frac{e_z(k+1) - e_z(k)}{t_s}. \tag{28}$$

From here, the dynamics error of $z(k)$ is generated as follows

$$e_z(k+1) = e_z(k) + t_s\dot{e}_z(k)$$
$$\dot{e}_z(k+1) = \frac{\dot{z}_d(k+1) - \dot{z}_d(k)}{t_s} + \dot{e}_z(k) + t_s\Big(-g + \delta_z(k) + (\cos\phi(k)\cos\theta(k))\frac{u_t(k)}{m}\Big). \tag{29}$$

Define the sliding surface of error dynamics of $z(k+1)$ as

$$S_z(k+1) = \lambda_z e_z(k+1) + \dot{e}_z(k+1), \tag{30}$$

where λ_z is a positive constant. If $S_z(k+1) = 0$, then

$$\frac{e_z(k+2) - e_z(k+1)}{t_s} = -\lambda_z e_z(k+1).$$

As a result

$$e_z(k+2) = (1 - t_s\lambda_z)e_z(k+1), \tag{31}$$

which implies that $e_z(k+1)$ exponentially converges to zero as $t \to \infty$ for any positive constant λ_z.

By substituting (29) to (30), hence

$$S_z(k+1) = \lambda_z e_z(k) + (t_s\lambda_z + 1)\dot{e}_z(k) + \frac{\dot{z}_d(k+1) - \dot{z}_d(k)}{t_s} + t_s\big(-g + \delta_z(k) + (\cos\phi(k)\cos\theta(k))\frac{u_t(k)}{m}\big). \tag{32}$$

Now, a robust control scheme using an extended TDSMC is designed to guarantee stability such that $S_z(k+1) \to 0$ as $t \to \infty$. The main result of this subsection is summarized in Theorem 1.

Theorem 1: Consider the dynamical model (21) under Assumption 1. The tracking control is guaranteed by selecting

$$u_t(k) = -\frac{m}{t_s\cos\phi(k)\cos\theta(k)}\Bigg(\lambda_z e_z(k) + (t_s\lambda_z + 1)\dot{e}_z(k) + \frac{\dot{z}_d(k+1) - \dot{z}_d(k)}{t_s} + t_s \times\Big(-g - \frac{k_{z_1}}{t_s}S_z(k) + k_{z_2}\tanh S_z(k)\Big)\Bigg), \tag{33}$$

where $k_{z_1} < -1$ and k_{z_2} are tuned such that

$$k_{z_2} > \frac{d_z(1 + k_{z_1})}{1 - k_{z_1}}, \quad \frac{t_s k_{z_2} - k_{z_1}}{t_s} > d_z, \tag{34}$$

for any $k_{z_1} \neq 0$ and $\lambda_z > 0$.

Proof: First, the controller is selected using the following conventional discrete-time sliding mode control (DTSMC)

$$u_t(k) = -\frac{m}{t_s\cos\phi(k)\cos\theta(k)}\Bigg(\lambda_z e_z(k) + (t_s\lambda_z + 1)\dot{e}_z(k) + \frac{\dot{z}_d(k+1) - \dot{z}_d(k)}{t_s}$$

$$+ t_s\Big(-g - \frac{k_{z_1}}{t_s}S_z(k) + k_{z_2}\text{sgn}S_z(k)\Big)\Big). \quad (35)$$

The system composed of (32) and (35) can be rewritten as

$$S_z(k+1) = t_s\Big(\delta_z(k) - k_{z2}\text{sgn}(S_z(k))\Big) + k_{z_1}S_z(k). \quad (36)$$

From (36), the following can be obtained

$$S_z(k+2) = t_s\Big(\delta_z(k+1) - k_{z_2}\text{sgn}(S_z(k+1))\Big) + k_{z_1}S_z(k+1). \quad (37)$$

Substituting (36) to (37), hence

$$\begin{aligned} S_z(k+2) &= t_s\Big(\delta_z(k+1) - k_{z_2}\text{sgn}(S_z(k+1))\Big) \\ &\quad + k_{z_1}^2 S_z(k) + t_s k_{z_1}\Big(\delta_z(k) - k_{z_2}\text{sgn}(S_z(k))\Big) \\ &= t_s\delta_z(k+1) - t_s k_{z_2}\text{sgn}(S_z(k+1)) \\ &\quad + k_{z_1}^2 S_z(k) + t_s k_{z_1}\delta_z(k) \\ &\quad - t_s k_{z_1}k_{z_2}\text{sgn}(S_z(k)). \end{aligned} \quad (38)$$

By following Gao's reaching law [12], the quasi-sliding motion (QSM) of the proposed design is shown by presenting the monotonous decrement of the absolute value of sliding surface $S_z(k+1)$ and the sliding surface trajectory stays in a specific band. The condition for QSM is

$$\text{sgn}(S_z(k+2)) = -S_z(k+1) = S_z(k). \quad (39)$$

The control gains k_{z_1} and k_{z_2} are selected to satisfy the QSM motion condition (39). Assume that $\text{sgn}(S_z(k+2)) = S_z(k) = 1$, from (38), the worst setting for $\text{sgn}(S_z(k+2))$ is under $\delta_z(k) = \delta_z(k+1) = -d_z$ for $S_z(k) \approx 0$ as expressed by

$$S_z(k+2) = -t_s(1+k_{z_1})d_z + t_s k_{z_2}(1-k_{z_1}). \quad (40)$$

The worst setting for $\text{sgn}(S_z(k+1))$ is under $\delta_z(k) = d_z$ as expressed by

$$S_z(k+1) = t_s d_z - t_s k_{z_2} + k_{z_1}. \quad (41)$$

By selecting $k_{z_1} < 1$ and k_{z_2} for any $k_{z_1} \neq 0$ such that (34) is satisfied. Then $S_z(k+2) > 0$ and $S_z(k+1) < 0$ is guaranteed.

As an undesirable phenomenon, chattering is a common problem in conventional SMC. Its oscillation has a finite amplitude and frequency that occurs around the desired equilibrium sliding surface [10]. Several methods have been proposed to handle this problem. However, the results for the discrete systems are still relatively rare in the literature. The non-smooth signum function in the control structure causes this problem. In this case, the function of the $\text{sgn}(S_z(k))$ has the following properties

$$\text{sgn}(S_z(k)) = \begin{cases} -1, & S_z(k) > 0 \\ 0, & \text{for } S_z(k) = 0 \\ 1, & S_z(k) < 0. \end{cases} \quad (42)$$

It means that the value of $\text{sgn}(S_z(k))$ is -1 or 1 for any $S_z(k) \neq 0$ regardless of the value of the sliding surface is negative big or negative small and vice versa. Integral SMC was proposed to attenuate high-frequency oscillation in [31]. However, this approach increases the sliding surface error and degrades the response systems. Another approach was developed in [33] for linear systems by proposing the aid of an exponentially decaying barrier Lyapunov function. More interesting results were investigated in [10] and [11] by approximating the value of the signum function to attenuate chattering. The performance and drawbacks of approximated functions were compared to verify their effectiveness. It can be concluded that the chattering can be attenuated by extending the boundary layer width. However, the robustness of the system may degrade due to a large boundary layer. Note that the aforementioned results were developed for continuous-time systems.

Inspired by [11], the chattering in DTQSMC is attenuated by approximating the value of the $\text{sgn}(S_z(k))$ using a hyperbolic tangent function $\tanh(S_z(k))$. Hence, the sign function in (35) is replaced by $\tanh(S_z(k))$ as represented by (33). This hyperbolic tangent function is a smooth function as expressed by

$$\tanh(S_z(k)) = \frac{e^{S_z(k)} - e^{-S_z(k)}}{e^{S_z(k)} + e^{-S_z(k)}}, \quad (43)$$

and contains the following properties

$$\tanh(S_z(k)) = \begin{cases} -1, & \text{for negative big } S_z(k) \\ 0, & \text{for } S_z(k) = 0 \\ 1, & \text{for positive big } S_z(k). \end{cases} \quad (44)$$

The proof is thus completed. ■

B. ROTATIONAL CONTROL DESIGN

In this subsection, a robust controller is designed for rotational dynamics in the discrete-time domain in the presence of external disturbances in time-varying form. The error position of rotational states is defined to be

$$\begin{aligned} e_\phi(k) &= \phi(k) - \phi_d(k) \\ e_\theta(k) &= \theta(k) - \theta_d(k) \\ e_\psi(k) &= \psi(k) - \psi_d(k). \end{aligned}$$

The error dynamics of (22), (23) and (24) are represented by

$$\begin{aligned} e_\phi(k+1) &= e_\phi(k) + t_s\dot{e}_\phi(k) \\ \dot{e}_\phi(k+1) &= \frac{\dot{\phi}_d(k+1) - \dot{\phi}_d(k)}{t_s} + \dot{e}_\phi(k) \\ &\quad + t_s\Big(w_\phi f_\phi(k) + \delta_\phi(k) + \frac{\tau_\phi(k)}{I_x}\Big) \end{aligned} \quad (45)$$

$$\begin{aligned} e_\theta(k+1) &= e_\theta(k) + t_s\dot{e}_\theta(k) \\ \dot{e}_\theta(k+1) &= \frac{\dot{\theta}_d(k+1) - \dot{\theta}_d(k)}{t_s} + \dot{e}_\theta(k) \\ &\quad + t_s\Big(w_\theta f_\theta(k) + \delta_\theta(k) + \frac{\tau_\theta(k)}{I_y}\Big) \end{aligned} \quad (46)$$

$$e_\psi(k+1) = e_\psi(k) + t_s\dot{e}_\psi(k)$$

$$\dot{e}_\psi(k+1) = \frac{\dot{\psi}_d(k+1) - \dot{\psi}_d(k)}{t_s} + \dot{e}_\psi(k) + t_s\left(w_\psi f_\psi(k) + \delta_\psi(k) + \frac{\tau_\psi(k)}{I_z}\right). \tag{47}$$

The sliding surface of error of rotational dynamics is defined as

$$S_\phi(k+1) = \lambda_\phi e_\phi(k+1) + \dot{e}_\phi(k+1) \tag{48}$$
$$S_\theta(k+1) = \lambda_\theta e_\theta(k+1) + \dot{e}_\theta(k+1) \tag{49}$$
$$S_\psi(k+1) = \lambda_\psi e_\psi(k+1) + \dot{e}_\psi(k+1), \tag{50}$$

where λ_ϕ, λ_θ and λ_ψ are some positive constants. If all $S_\phi(k+1)$, $S_\theta(k+1)$ and $S_\psi(k+1)$ are zero, then

$$\frac{e_\phi(k+2) - e_\phi(k+1)}{t_s} = -\lambda_\phi e_\phi(k+1)$$
$$\frac{e_\theta(k+2) - e_\theta(k+1)}{t_s} = -\lambda_\theta e_\theta(k+1)$$
$$\frac{e_\psi(k+2) - e_\psi(k+1)}{t_s} = -\lambda_\psi e_\psi(k+1).$$

As results

$$e_\phi(k+2) = (1 - t_s\lambda_\phi)e_\phi(k+1) \tag{51}$$
$$e_\theta(k+2) = (1 - t_s\lambda_\theta)e_\theta(k+1) \tag{52}$$
$$e_\psi(k+2) = (1 - t_s\lambda_\psi)e_\psi(k+1), \tag{53}$$

which imply that $e_\phi(k+1)$, $e_\theta(k+1)$ and $e_\psi(k+1)$ exponentially converge to zero as $t \to \infty$ for some positive constants λ_ϕ, λ_θ and λ_ψ.

By substituting (45), (46) and (47) to (48), (49) and (50), respectively, then

$$S_\phi(k+1) = \lambda_\phi e_\phi(k) + (t_s\lambda_\phi + 1)\dot{e}_\phi(k) + \frac{\dot{\phi}_d(k+1) - \dot{\phi}_d(k)}{t_s} + t_s\Big(w_\phi f_\phi(k) + \delta_\phi(k) + \frac{\tau_\phi(k)}{I_x}\Big) \tag{54}$$

$$S_\theta(k+1) = \lambda_\theta e_\theta(k) + (t_s\lambda_\theta + 1)\dot{e}_\theta(k) + \frac{\dot{\theta}_d(k+1) - \dot{\theta}_d(k)}{t_s} + t_s\Big(w_\theta f_\theta(k) + \delta_\theta(k) + \frac{\tau_\theta(k)}{I_x}\Big) \tag{55}$$

$$S_\psi(k+1) = \lambda_\psi e_\psi(k) + (t_s\lambda_\psi + 1)\dot{e}_\psi(k) + \frac{\dot{\psi}_d(k+1) - \dot{\psi}_d(k)}{t_s} + t_s\Big(w_\psi f_\psi(k) + \delta_\psi(k) + \frac{\tau_\psi(k)}{I_x}\Big). \tag{56}$$

Now, a robust control scheme using an extended DTQSMC is designed to guarantee stability such that $S_\phi(k+1) \to 0$, $S_\theta(k+1) \to 0$ and $S_\psi(k+1) \to 0$ as $t \to \infty$. The proposed control design for rotational dynamics is summarized in Theorem 2.

Theorem 2: Consider the rotational dynamics (22), (23) and (24) under Assumption 1. The tracking control is guaranteed by selecting

$$\tau_\phi(k) = -\frac{I_x}{t_s}\bigg(\lambda_\phi e_\phi(k) + (t_s\lambda_\phi + 1)\dot{e}_\phi(k) + \frac{\dot{\phi}_d(k+1) - \dot{\phi}_d(k)}{t_s} + t_s\Big(w_\phi f_\phi(k) - \frac{k_{\phi_1}}{t_s}S_\phi(k) + k_{\phi_2}\tanh S_\phi(k)\Big)\bigg) \tag{57}$$

$$\tau_\theta(k) = -\frac{I_y}{t_s}\bigg(\lambda_\theta e_\theta(k) + (t_s\lambda_\theta + 1)\dot{e}_\theta(k) + \frac{\dot{\theta}_d(k+1) - \dot{\theta}_d(k)}{t_s} + t_s\Big(w_\theta f_\theta(k) - \frac{k_{\phi_1}}{t_s}S_\phi(k) + k_{\phi_2}\tanh S_\phi(k)\Big)\bigg) \tag{58}$$

$$\tau_\psi(k) = -\frac{I_z}{t_s}\bigg(\lambda_\psi e_\psi(k) + (t_s\lambda_\psi + 1)\dot{e}_\psi(k) + \frac{\dot{\psi}_d(k+1) - \dot{\psi}_d(k)}{t_s} + t_s\Big(w_\psi f_\psi(k) - \frac{k_{\psi_1}}{t_s}S_\psi(k) + k_{\psi_2}\tanh S_\psi(k)\Big)\bigg), \tag{59}$$

where both $k_{\phi_1} < 1$, k_{ϕ_2}, $k_{\theta_1} < 1$, k_{θ_2}, $k_{\psi_1} < 1$ and k_{ψ_2} are selected such that where $k_{z_1} < 1$ and k_{z_2} are tuned such that

$$k_{\phi_2} > \frac{d_\phi(1 + k_{\phi_1})}{1 - k_{\phi_1}}, \quad \frac{t_s k_{\phi_2} - k_{\phi_1}}{t_s} > d_\phi, \ \lambda_\phi > 0 \tag{60}$$
$$k_{\theta_2} > \frac{d_\theta(1 + k_{\theta_1})}{1 - k_{\theta_1}}, \quad \frac{t_s k_{\theta_2} - k_{\theta_1}}{t_s} > d_\theta, \ \lambda_\theta > 0 \tag{61}$$
$$k_{\psi_2} > \frac{d_\psi(1 + k_{\psi_1})}{1 - k_{\psi_1}}, \quad \frac{t_s k_{\psi_2} - k_{\psi_1}}{t_s} > d_\psi, \ \lambda_\psi > 0, \tag{62}$$

for any non-zero k_{ϕ_1}, k_{θ_1} and k_{ψ_1}.

Proof: In the first step, the controller is selected using the following conventional DTSMC

$$\tau_\phi(k) = -\frac{I_x}{t_s}\bigg(\lambda_\phi e_\phi(k) + (t_s\lambda_\phi + 1)\dot{e}_\phi(k) + \frac{\dot{\phi}_d(k+1) - \dot{\phi}_d(k)}{t_s} + t_s\Big(w_\phi f_\phi(k) - \frac{k_{\phi_1}}{t_s}S_\phi(k) + k_{\phi_2}\text{sgn}S_\phi(k)\Big)\bigg) \tag{63}$$

$$\tau_\theta(k) = -\frac{I_y}{t_s}\bigg(\lambda_\theta e_\theta(k) + (t_s\lambda_\theta + 1)\dot{e}_\theta(k) + \frac{\dot{\theta}_d(k+1) - \dot{\theta}_d(k)}{t_s} + t_s\Big(w_\theta f_\theta(k) - \frac{k_{\phi_1}}{t_s}S_\phi(k) + k_{\phi_2}\text{sgn}S_\phi(k)\Big)\bigg) \tag{64}$$

$$\tau_\psi(k) = -\frac{I_z}{t_s}\bigg(\lambda_\psi e_\psi(k) + (t_s\lambda_\psi + 1)\dot{e}_\psi(k) + \frac{\dot{\psi}_d(k+1) - \dot{\psi}_d(k)}{t_s} + t_s\Big(w_\psi f_\psi(k)$$

$$-\frac{k_{\psi_1}}{t_s}S_\psi(k)+k_{\psi_2}\text{sgn}S_\psi(k)\Big)\Big). \quad (65)$$

The closed-loop systems composed of (54), (55), (56), (63), (64) and (65) can be rewritten as

$$S_\phi(k+1)=t_s\Big(\delta_\phi(k)-k_{\phi_2}\text{sgn}(S_\phi(k))\Big)+k_{\phi_1}S_\phi(k) \quad (66)$$
$$S_\theta(k+1)=t_s\Big(\delta_\theta(k)-k_{\theta_2}\text{sgn}(S_\theta(k))\Big)+k_{\theta_1}S_\theta(k) \quad (67)$$
$$S_\psi(k+1)=t_s\Big(\delta_\psi(k)-k_{\psi_2}\text{sgn}(S_\psi(k))\Big)+k_{\psi_1}S_\psi(k). \quad (68)$$

From (66), (67) and (68), it can be generated

$$S_\phi(k+2)=t_s\lambda_\phi\Big(\delta_\phi(k+1)-k_{\phi_2}\text{sgn}(S_\phi(k+1))\Big)+k_{\phi_1}S_\phi(k+1) \quad (69)$$
$$S_\theta(k+2)=t_s\lambda_\theta\Big(\delta_\theta(k+1)-k_{\theta_2}\text{sgn}(S_\theta(k+1))\Big)+k_{\theta_1}S_\theta(k+1) \quad (70)$$
$$S_\psi(k+2)=t_s\lambda_\psi\Big(\delta_\psi(k+1)-k_{\psi_2}\text{sgn}(S_\psi(k+1))\Big)+k_{\psi_1}S_\psi(k+1). \quad (71)$$

Substituting (66), (67) and (68) to (69), (70) and (71), respectively. Then the following can be obtained

$$S_\phi(k+2)=t_s\delta_\phi(k+1)-t_sk_{\phi_2}\text{sgn}(S_\phi(k+1))+k_{\phi_1}^2S_\phi(k)+t_sk_{\phi_1}\delta_\phi(k)-t_sk_{\phi_1}k_{\phi_2}\text{sgn}(S_z(k)) \quad (72)$$
$$S_\theta(k+2)=t_s\delta_\theta(k+1)-t_sk_{\theta_2}\text{sgn}(S_\theta(k+1))+k_{\theta_1}^2S_\theta(k)+t_sk_{\theta_1}\delta_\theta(k)-t_sk_{\theta_1}k_{\theta_2}\text{sgn}(S_\theta(k)) \quad (73)$$
$$S_\psi(k+2)=t_s\delta_\psi(k+1)-t_sk_{\psi_2}\text{sgn}(S_\psi(k+1))+k_{\psi_1}^2S_\psi(k)+t_sk_{\psi_1}\delta_\psi(k)-t_sk_{\psi_1}k_{\psi_2}\text{sgn}(S_\psi(k)). \quad (74)$$

By following Gao's reaching law [12], the quasi-sliding motion (QSM) of the proposed design is shown by presenting the monotonous decrement of the absolute value of sliding surface $S_z(k+1)$ and the sliding surface trajectory stays in a specific band. The condition for QSM is

$$\text{sgn}(S_\phi(k+2))=-S_\phi(k+1)=S_\phi(k) \quad (75)$$
$$\text{sgn}(S_\theta(k+2))=-S_\theta(k+1)=S_\theta(k) \quad (76)$$
$$\text{sgn}(S_\psi(k+2))=-S_\psi(k+1)=S_\psi(k). \quad (77)$$

Now, the control gains k_{ϕ_1}, k_{ϕ_2}, k_{θ_1}, k_{θ_2}, k_{ψ_1} and k_{ψ_2} is calculated to satisfy the QSM motion conditions (75), (76) and (77). Assume that $\text{sgn}(S_\phi(k+2)) = \text{sgn}((S_\phi(k)) = \text{sgn}(S_\theta(k+2)) = S_\theta(k) = \text{sgn}(S_\psi(k+2)) = S_\psi(k) = 1$. From (72), (73) and (74), The worst scenarios for $\text{sgn}(S_\phi(k+2))$, $\text{sgn}(S_\theta(k+2))$ and $\text{sgn}(S_\psi(k+2))$, respectively are

$$\delta_\phi(k)=\delta_\phi(k+1)=-d_\phi,\quad S_\phi(k)\approx 0$$
$$\delta_\theta(k)=\delta_\theta(k+1)=-d_\theta,\quad S_\theta(k)\approx 0$$
$$\delta_\psi(k)=\delta_\psi(k+1)=-d_\psi,\quad S_\psi(k)\approx 0.$$

TABLE 1. The parameters of a VTOL UAV [13].

Parameter name	Notation	Value
Mass	m	$3\ kg$
Gravity acceleration	g	$9.81\ m/s^2$
Inertia of x-axis	I_x	$3.0671\ kg.m^2$
Inertia of y-axis	I_y	$3.0671\ kg.m^2$
Inertia of z-axis	I_z	$12.579\ g.m^2$

As results

$$S_\phi(k+2)=-t_s(1+k_{\phi_1})d_\phi+t_sk_{\phi_2}(1-k_{\phi_1}) \quad (78)$$
$$S_\theta(k+2)=-t_s(1+k_{\theta_1})d_\theta+t_sk_{\theta_2}(1-k_{\theta_1}) \quad (79)$$
$$S_\psi(k+2)=-t_s(1+k_{\psi_1})d_\psi+t_sk_{\psi_2}(1-k_{\psi_1}). \quad (80)$$

In another side, the worst setting for $\text{sgn}(S_\phi(k+1))$, $\text{sgn}(S_\theta(k+1))$ and $\text{sgn}(S_\psi(k+1))$ are

$$\delta_\phi(k)=d_\phi,\quad \delta_\theta(k)=d_\theta,\quad \delta_\psi(k)=d_\psi.$$

Hence

$$S_\phi(k+1)=t_sd_\phi-t_sk_{\phi_2}+k_{\phi_1} \quad (81)$$
$$S_\theta(k+1)=t_sd_\theta-t_sk_{\theta_2}+k_{\theta_1} \quad (82)$$
$$S_\psi(k+1)=t_sd_\psi-t_sk_{\psi_2}+k_{\psi_1}. \quad (83)$$

By selecting $k_{\phi_1} < 1, k_{\phi_2}, k_{\theta_1} < 1, k_{\theta_2}, k_{\psi_1} < 1$ and k_{ψ_2} for any non-zero k_{ϕ_1}, k_{θ_1} and k_{ψ_1} such that (60), (61) and (62) are satisfied. The following can be guaranteed

$$S_\phi(k+2)>0,\quad S_\phi(k+1)<0$$
$$S_\theta(k+2)>0,\quad S_\theta(k+1)<0$$
$$S_\psi(k+2)>0,\quad S_\psi(k+1)<0.$$

Similar to translational controller design, the values of the $\text{sgn}(S_\phi(k))$, $\text{sgn}(S_\theta(k))$ and $\text{sgn}(S_\psi(k))$ are approximated using the hyperbolic tangent functions $\tanh(S_\phi(k))$, $\tanh(S_\theta(k))$ and $\tanh(S_\psi(k))$, respectively, to reduce the chattering in DTQSMC. Hence, the sign function in (63), (64) and (65) are replaced by $\tanh(S_\phi(k))$, $\tanh(S_\theta(k))$ and $\tanh(S_\psi(k))$ as represented by (57), (58) and (59), respectively . The proof is thus completed. ■

IV. SIMULATION RESULTS

Some simulations are presented in Matlab/Simulink to evaluate numerically the proposed controller for VTOL UAV. The parameters used are listed in Table 1.

The external disturbance is added as follows

$$\delta_z=0.1\sin t,\quad \delta_\phi=0.1\sin t$$
$$\delta_\theta=0.12\cos t,\quad \delta_\psi=0.06\cos t.$$

The extended quasi-sliding mode control (QSMC) schemes for both translational and rotational dynamics are designed according to Theorem 1 and 2. The gains are selected as follows

$$\lambda_{x_1}=1,\quad \lambda_{x_2}=10^{-4},\quad \lambda_{y_1}=1,\quad \lambda_{y_2}=10^{-4}$$

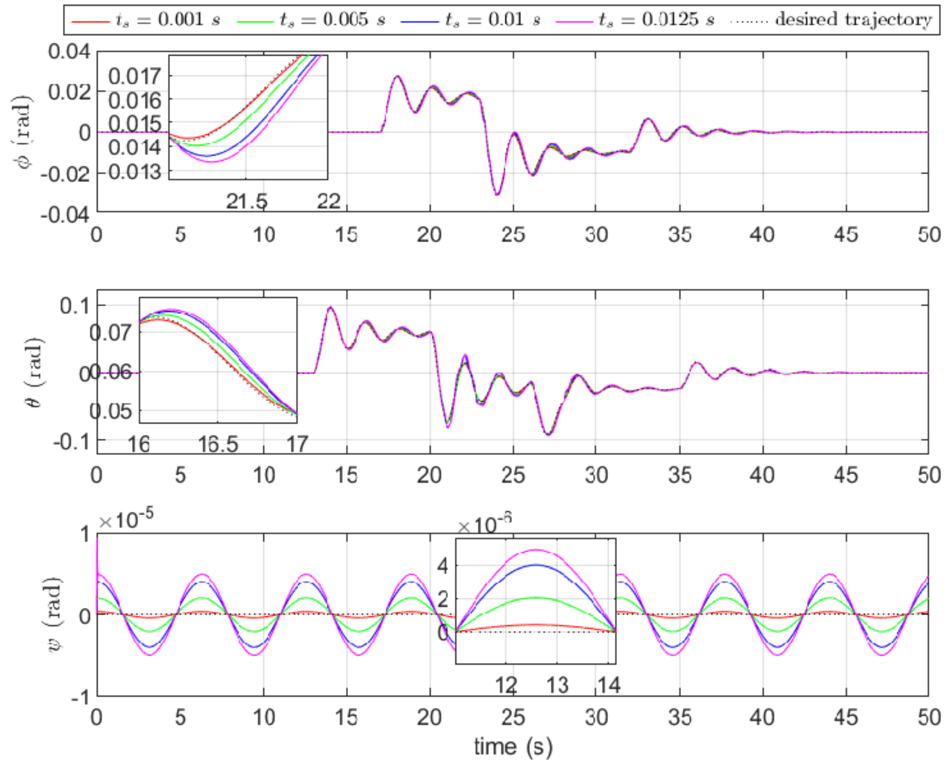

FIGURE 2. Profile of ϕ, θ and ψ.

$$
\begin{aligned}
k_{z_1} &= -10^{-5}, \quad k_{z_2} = 1, \quad \lambda_z = 50 \\
k_{\phi_1} &= -0.5, \quad k_{\phi_2} = 5, \quad \lambda_\phi = 100 \\
k_{\theta_1} &= -0.5, \quad k_{\theta_2} = 10, \quad \lambda_\theta = 90 \\
k_{\psi_1} &= -0.5, \quad k_{\psi_2} = 7, \quad \lambda_\psi = 95. \qquad (84)
\end{aligned}
$$

To demonstrate the real application setting, the value of total thrust u_t is set to be between $-60\ kg{\cdot}m/s^2$ to $60\ kg{\cdot}m/s^2$. In another side, the values of τ_ϕ, τ_θ and τ_ψ are limited from $-2\ kg \cdot m^2/s^2$ to $2\ kg \cdot m^2/s^2$. The simulation results using the proposed controller are illustrated in Figures 2-5. Some simulations are conducted with four different time sampling. It can be seen that the proposed design is able to drive all states to follow the desired VTOL trajectories, as presented in Figures 2 and 3. The proposed scheme has robust terms that can guarantee the convergence of VTOL UAV states to the desired path.

Figure 3 illustrates the position of VTOL UAV with respect to x, y, and z axes. It can be seen that the aircraft takes off from initial position $\eta_1(0) = [0\ 0\ 0]^{\mathsf{T}}$ and requires around 10 s for VTOL UAV to reach the highest desired altitude. After hovering 3 s, it moves in x and y directions and performs vertical landing is conducted from $t = 40\ s$ to $t = 50\ s$. This movement is plotted in 3D in Figure 5. Also, all orientation angles can follow the desired trajectory as presented in Figure 2. The initial position of orientations angles is $\eta_2(0) = [0\ 0\ 0]^{\mathsf{T}}$. While Figure 4 shows control inputs applied to maintain VTOL UAV movement. It can be seen in Figures 2 and 3 that the chattering problem commonly appearing in conventional SMC is significantly reduced using the proposed control design. These results verify the performance of the controller developed in Theorem 1 and 2.

TABLE 2. The fitness of VTOL UAV states.

State	$t_s = 0.001\ s$	$t_s = 0.005\ s$	$t_s = 0.01\ s$	$t_s = 0.0125\ s$
ϕ	97.801%	96.670%	95.192%	94.374%
θ	97.708%	96.725%	95.318%	94.728%
x	99.483%	99.493%	99.503%	99.510%
y	99.356%	99.367%	99.380%	99.387%
z	99.916%	99.914%	99.912%	99.910%
Average	98.853%	98.434%	97.861%	97.582%

To have a better presentation, the fitness of all states can be calculated using the following formula

$$
\text{fitness of state}(\%) = 100\left(1 - \frac{\|\text{desired state} - \text{state}\|}{\|\text{desired state}\|}\right). \qquad (85)
$$

The fitness of all states for every time sampling is listed in Table 2.

The proposed scheme to handle the VTOL UAV motion is differentiated by conducting simulations in different t_s, as presented in Table 2. It shows that the tracking control of all states has outstanding fitness. The fitness average of all states is slightly decreasing for a higher t_s. Note that the fitness of ψ cannot be calculated as ϕ_d is zero. However, it can be seen from Figure 2 that the tracking control for VTOL UAV with smaller t_s is slightly better.

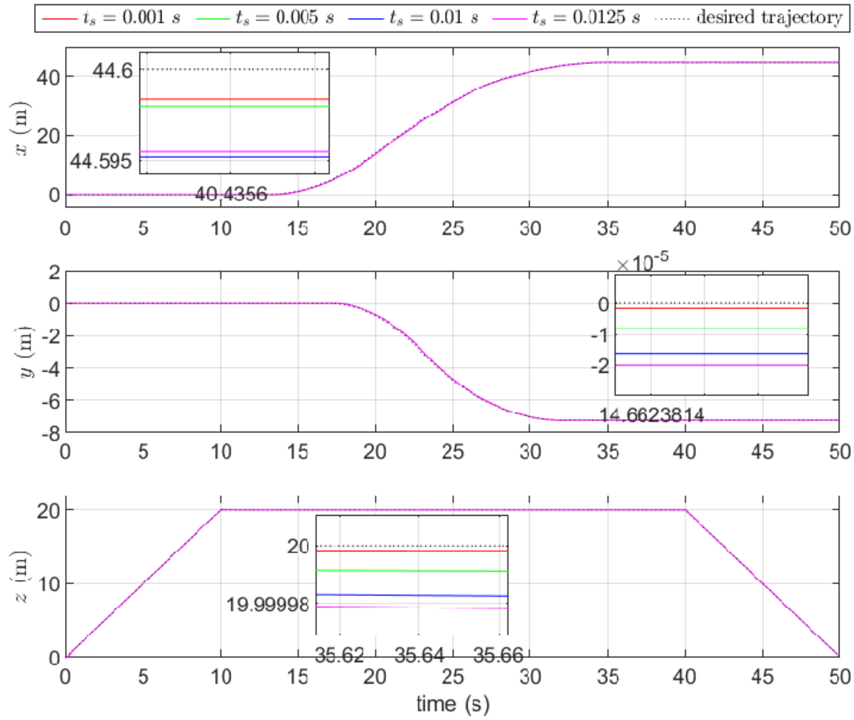

FIGURE 3. Profile of x, y and z.

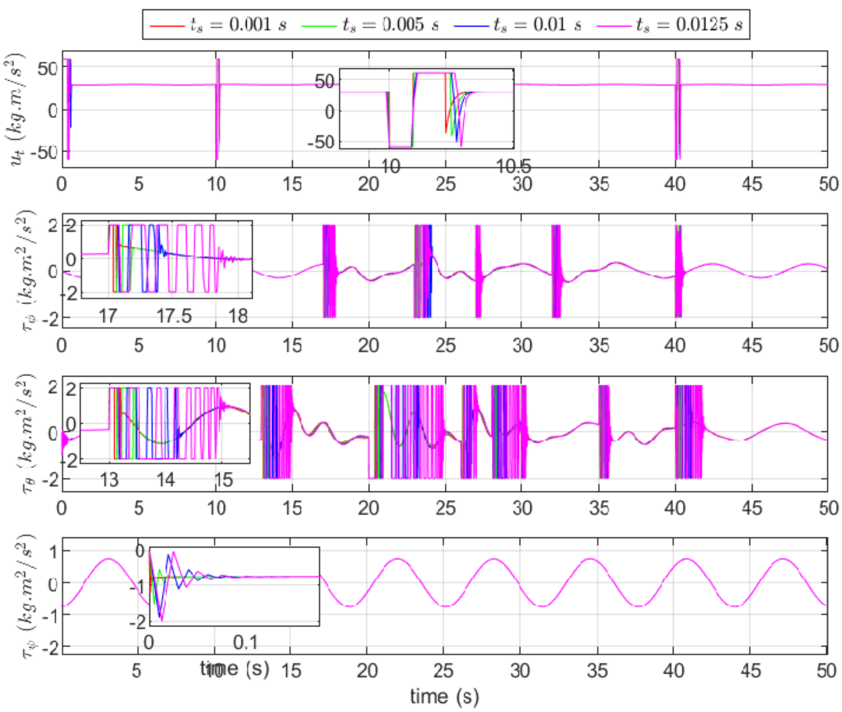

FIGURE 4. Profile of u_t and τ.

To evaluate the sensitivity of the control parameters, the gains (84) are reduced 50% such that

$$\lambda_{x_1} = 0.5, \quad \lambda_{x_2} = 5 \times 10^{-5}, \ \lambda_{y_1} = 0.5, \ \lambda_{y_2} = 5 \times 10^{-5}$$
$$k_{z_1} = -5 \times 10^{-6}, \quad k_{z_2} = 0.5, \ \lambda_z = 25$$
$$k_{\phi_1} = -0.25, \quad k_{\phi_2} = 2.5, \ \lambda_\phi = 50$$
$$k_{\theta_1} = -0.25, \quad k_{\theta_2} = 5, \ \lambda_\theta = 45$$
$$k_{\psi_1} = -0.25, \quad k_{\psi_2} = 3.5, \ \lambda_\psi = 47.5. \tag{86}$$

Similar to the previous setting, the value of total thrust u_t is between $-60\ kg.m/s^2$ to $60\ kg.m/s^2$, and all of the torques are limited from $-2\ kg.m^2/s^2$ to $2\ kg.m^2/s^2$. The proposed

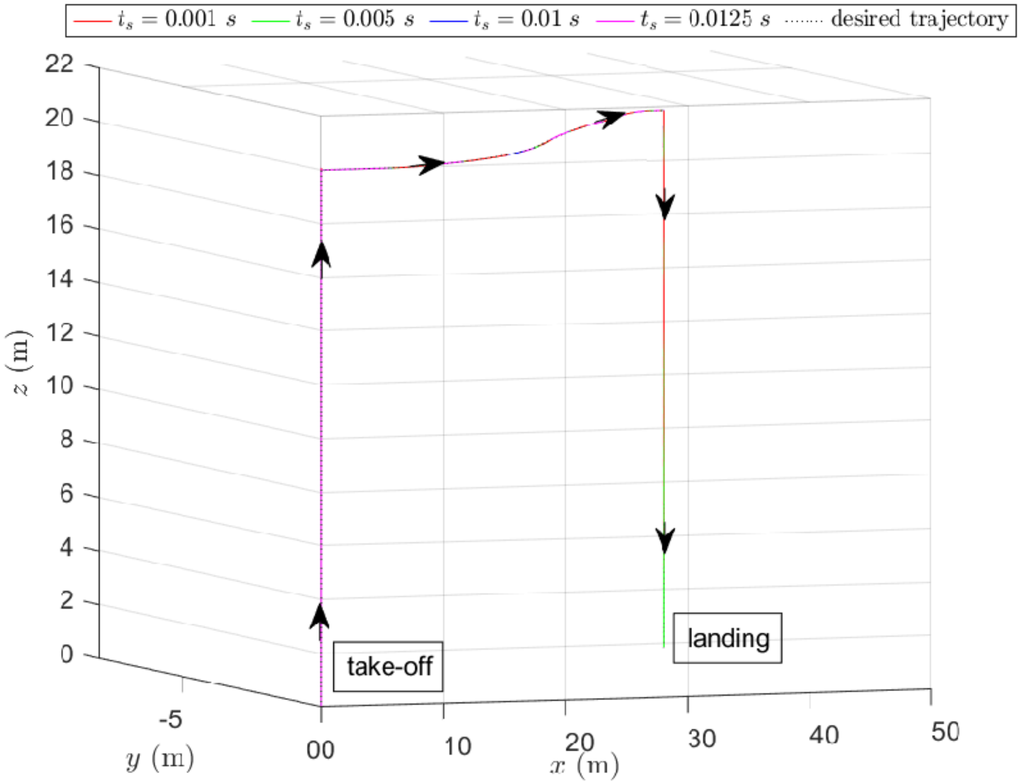

FIGURE 5. Profile of x, y and z in 3D.

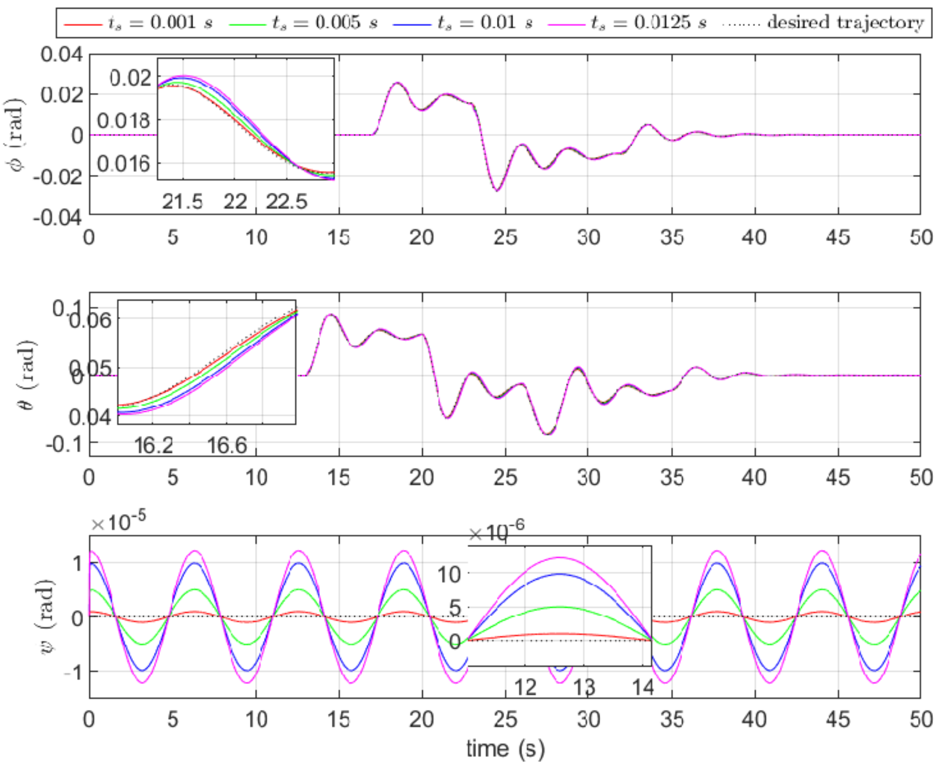

FIGURE 6. Profile of ϕ, θ and ψ under gains in equation (86).

control design still shows outstanding performance as illustrated in Figures 6-9. Figure 6 shows tracking control of every attitude or rotational states i.e. ϕ, θ, and ψ. Position tracking performance with respect to x, y, and z axes is illustrated

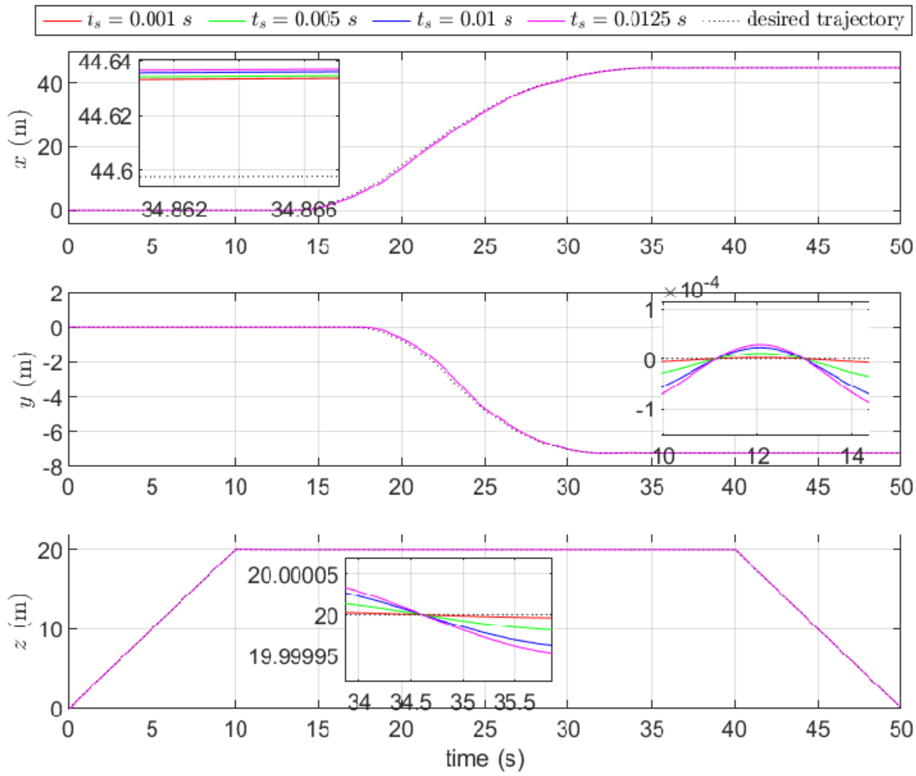

FIGURE 7. Profile of x, y and z under gains in equation (86).

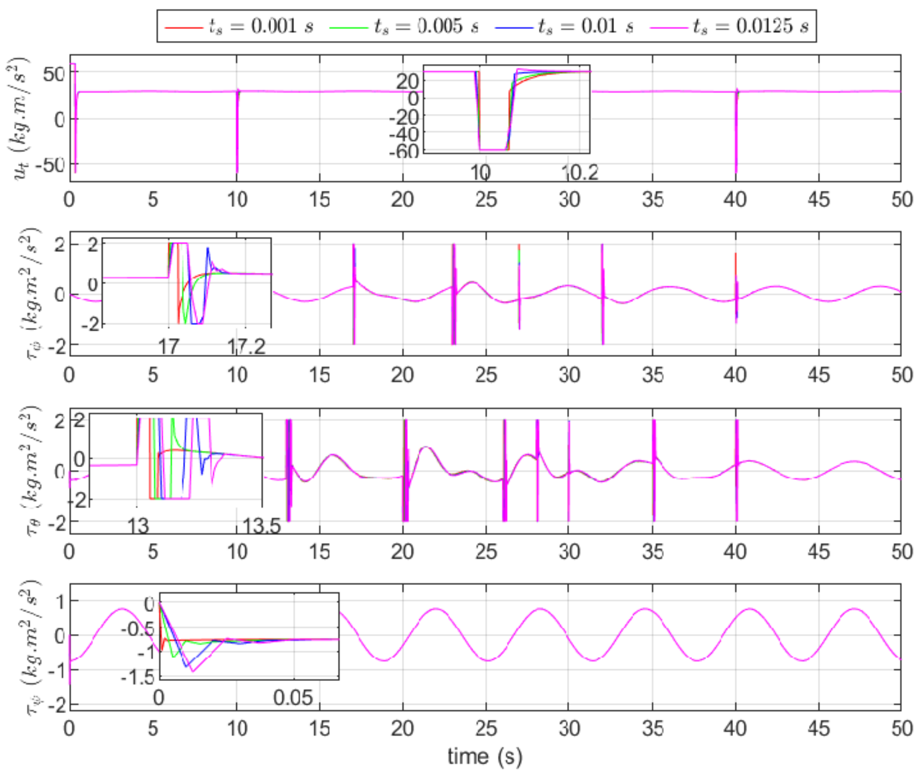

FIGURE 8. Profile of u_t and τ under gains in equation (86).

in Figures 7 and 9. Also, Figures 6 and 7 confirm that the chattering issue in every state of VTOL UAV is significantly reduced as concluded by the proposed control design in Section III. The fitness of all states is also calculated

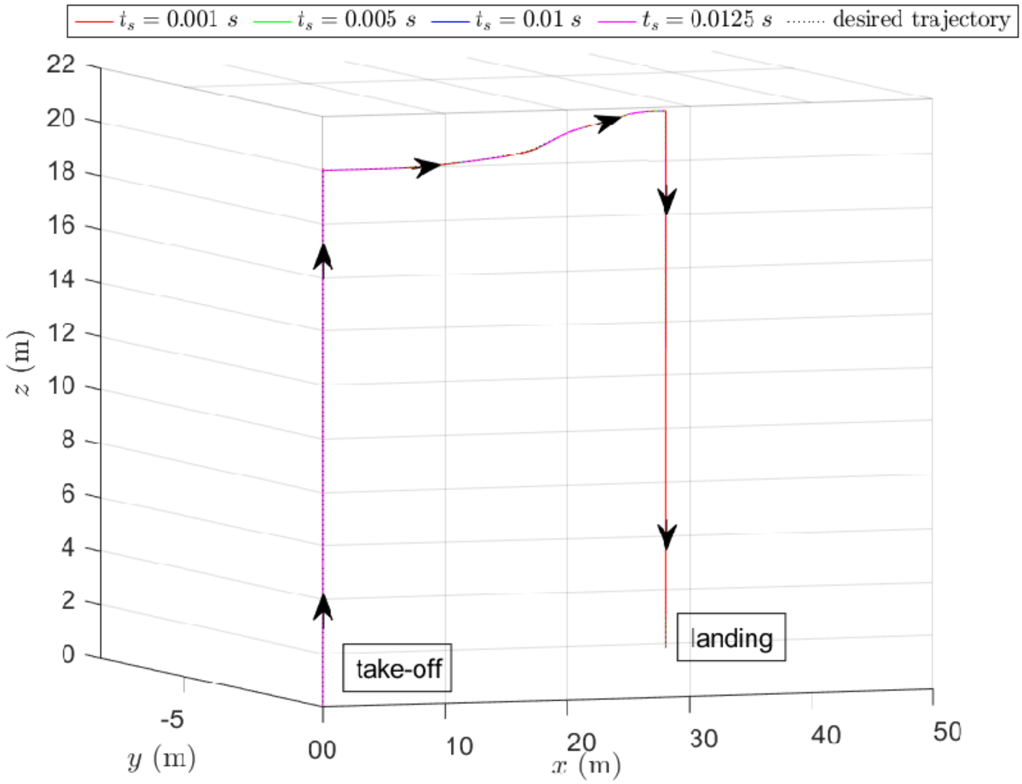

FIGURE 9. Profile of x, y and z in 3D under gains in equation (86).

TABLE 3. The fitness of VTOL UAV states under gains (86).

State	$t_s = 0.001\ s$	$t_s = 0.005\ s$	$t_s = 0.01\ s$	$t_s = 0.0125\ s$
ϕ	97.733%	97.111%	96.264%	95.867%
θ	97.528%	96.901%	96.073%	95.650%
x	98.957%	98.966%	98.978%	98.985%
y	98.701%	98.712%	98.726%	98.733%
z	99.895%	99.893%	99.891%	99.890%
Average	98.563%	98.317%	97.986%	97.825%

using (85) listed in Table 3. It shows that the proposed controller still has excellent performance to maintain the tracking control stability in various time sampling.

V. CONCLUSION

This paper studied a fully robust discrete tracking control for 6-DOF VTOL UAV in the presence of uncertain time-varying disturbances. Discrete tracking control for translational and rotational motions was designed using an extended QSMC. The chattering issue in the conventional SMC was reduced in the proposed design. A new reaching law for VTOL UAV was developed to guarantee tracking control stability in the discrete-time domain. A rigorous mathematical analysis was presented to prove the tracking control stability of the proposed design. Several simulations were conducted with different time sampling to verify the performance of the proposed approaches. Implementing this design for real VTOL UAV applications will be interesting in future works.

REFERENCES

[1] J. U. Alvarez-Muñoz, J. A. Escareno, J. Chevalier, S. Daix, and O. Labanni-Igbida, ''Wind-tolerant event-based adaptive sliding-mode control for VTOL rotorcrafts multiagent systems,'' *IEEE Trans. Aerosp. Electron. Syst.*, vol. 59, no. 2, pp. 1400–1410, Apr. 2023.

[2] B. D. O. Anderson, ''Failures of adaptive control theory and their resolution,'' *Commun. Inf. Syst.*, vol. 5, no. 1, pp. 1–20, 2005.

[3] A. Astolfi, D. Karagiannis, and R. Ortega, *Nonlinear and Adaptive Control With Applications*. Cham, Switzerland: Springer, 2007.

[4] S. Bouabdallah, P. Murrieri, and R. Siegwart, ''Design and control of an indoor micro quadrotor,'' in *Proc. IEEE Int. Conf. Robot. Autom.*, 2004, pp. 4393–4398.

[5] K. Chen and A. Astolfi, ''I&I adaptive control for systems with varying parameters,'' in *Proc. IEEE Conf. Decis. Control (CDC)*, 2018, pp. 2205–2210.

[6] K. Chen and A. Astolfi, ''Adaptive control for systems with time-varying parameters,'' *IEEE Trans. Autom. Control*, vol. 66, no. 5, pp. 1986–2001, May 2021.

[7] A. Das and F. L. Lewis, ''Distributed adaptive control for synchronization of unknown nonlinear networked systems,'' *Automatica*, vol. 46, no. 12, pp. 2014–2021, Dec. 2010.

[8] A. Das and F. L. Lewis, ''Cooperative adaptive control for synchronization of second-order systems with unknown nonlinearities,'' *Int. J. Robust Nonlinear Control*, vol. 21, no. 13, pp. 1509–1524, Sep. 2011.

[9] G. J. J. Ducard and M. Allenspach, ''Review of designs and flight control techniques of hybrid and convertible VTOL UAVs,'' *Aerosp. Sci. Technol.*, vol. 118, Nov. 2021, Art. no. 107035.

[10] A. Eltayeb, M. F. Rahmat, M. A. M. Basri, and M. S. Mahmoud, ''An improved design of integral sliding mode controller for chattering attenuation and trajectory tracking of the quadrotor UAV,'' *Arabian J. Sci. Eng.*, vol. 45, no. 8, pp. 6949–6961, Aug. 2020.

[11] A. Eltayeb, M. F. Rahmat, M. A. M. Basri, M. A. M. Eltoum, and M. S. Mahmoud, ''Integral adaptive sliding mode control for quadcopter UAV under variable payload and disturbance,'' *IEEE Access*, vol. 10, pp. 94754–94764, 2022.

[12] W. Gao, Y. Wang, and A. Homaifa, "Discrete-time variable structure control systems," *IEEE Trans. Ind. Electron.*, vol. 42, no. 2, pp. 117–122, Apr. 1995.
[13] A. Guclu, "Designing autopilot and guidance algorithms to control translational and rotational dynamics of a fixed wing VTOL UAV," Ph.D. thesis, Dept. Aerosp. Eng., Middle East Tech. Univ., Ankara, Türkiye, 2020.
[14] A. Guclu, D. F. Kurtulus, and K. B. Arikan, "Attitude and altitude stabilization of fixed wing VTOL unmanned air vehicle," in *Proc. AIAA Modeling Simulation Technol. Conf.*, Jun. 2016, p. 3378.
[15] A. He, Y. Zhang, H. Zhao, B. Wang, and Z. Gao, "Adaptive fault-tolerant control of a hybrid VTOL UAV against actuator faults and model uncertainties under fixed-wing mode," *Int. J. Aerosp. Eng.*, vol. 2022, pp. 1–11, Jan. 2022.
[16] G. V. Hollweg, P. J. D. de Oliveira Evald, D. M. C. Milbradt, R. V. Tambara, and H. A. Gründling, "Lyapunov stability analysis of discrete-time robust adaptive super-twisting sliding mode controller," *Int. J. Control*, vol. 96, no. 3, pp. 614–627, Mar. 2023.
[17] N. Hovakimyan and C. Cao, *$\mathcal{L}_1$ Adaptive Control Theory: Guaranteed Robustness With Fast Adaptation*, vol. 21. Philadelphia, PA, USA: SIAM, 2010.
[18] Y. Hu, J. Guo, P. Ying, G. Zeng, and N. Chen, "Nonlinear control of a single tail tilt servomotor tri-rotor ducted VTOL-UAV," *Aerospace*, vol. 9, no. 6, p. 296, May 2022.
[19] T. Huang, D. Huang, Z. Wang, and A. Shah, "Robust tracking control of a quadrotor UAV based on adaptive sliding mode controller," *Complexity*, vol. 2019, pp. 1–15, Dec. 2019.
[20] I. H. Imran and A. Montazeri, "An adaptive scheme to estimate unknown parameters of an unmanned aerial vehicle," in *Proc. Int. Conf. Nonlinearity, Inf. Robot. (NIR)*, Dec. 2020, pp. 1–6.
[21] I. H. Imran, Z. Chen, L. Zhu, and M. Fu, "A distributed adaptive scheme for multiagent systems," *Asian J. Control*, vol. 24, no. 1, pp. 46–57, Jan. 2022.
[22] I. H. Imran, R. Stolkin, and A. Montazeri, "Adaptive control of quadrotor unmanned aerial vehicle with time-varying uncertainties," *IEEE Access*, vol. 11, pp. 19710–19724, 2023.
[23] D. Lee, A. Awan, S. Kim, and H. J. Kim, "Adaptive control for a VTOL UAV operating near a wall," in *Proc. AIAA Guid., Navigat., Control Conf.*, Aug. 2012, p. 4835.
[24] S. Li, Y. Wang, J. Tan, and Y. Zheng, "Adaptive RBFNNs/integral sliding mode control for a quadrotor aircraft," *Neurocomputing*, vol. 216, pp. 126–134, Dec. 2016.
[25] X. Liu, R. Ortega, H. Su, and J. Chu, "Immersion and invariance adaptive control of nonlinearly parameterized nonlinear systems," *IEEE Trans. Autom. Control*, vol. 55, no. 9, pp. 2209–2214, Sep. 2010.
[26] X. Lyu, J. Zhou, H. Gu, Z. Li, S. Shen, and F. Zhang, "Disturbance observer based hovering control of quadrotor tail-sitter VTOL UAVs using H_∞ synthesis," *IEEE Robot. Autom. Lett.*, vol. 3, no. 4, pp. 2910–2917, Oct. 2018.
[27] A. Montazeri, C. West, S. D. Monk, and C. J. Taylor, "Dynamic modelling and parameter estimation of a hydraulic robot manipulator using a multi-objective genetic algorithm," *Int. J. Control*, vol. 90, no. 4, pp. 661–683, Apr. 2017.
[28] A. Montazeri, A. Can, and I. H. Imran, "Unmanned aerial systems: Autonomy, cognition and control," in *Unmanned Aerial Systems: Theoretical Foundation and Applications*. Amsterdam, The Netherlands: Elsevier, 2020.
[29] Y. Mousavi, A. Zarei, A. Mousavi, and M. Biari, "Robust optimal higher-order-observer-based dynamic sliding mode control for VTOL unmanned aerial vehicles," *Int. J. Autom. Comput.*, vol. 18, no. 5, pp. 802–813, Oct. 2021.
[30] K. S. Narendra and A. M. Annaswamy, *Stable Adaptive Systems*. Upper Saddle River, NJ, USA: Prentice-Hall, 1989.
[31] A. Sahamijoo, F. Piltan, M. H. Mazloom, M. R. Avazpour, H. Ghiasi, and N. B. Sulaiman, "Methodologies of chattering attenuation in sliding mode controller," *Int. J. Hybrid Inf. Technol.*, vol. 9, no. 2, pp. 11–36, Feb. 2016.
[32] J. Samantaray and S. Chakrabarty, "Discrete time sliding mode control," in *Control Theory in Engineering*. London, U.K.: IntechOpen, 2020, p. 101.
[33] W. Tu and J. Dong, "Reduced-order robust nonlinear sliding mode fault-tolerant control for linear systems with disturbances: A prescribed practical sliding surface approach," *Int. J. Robust Nonlinear Control*, vol. 2020, pp. 1–10, Jun. 2022.
[34] H. Voos, "Nonlinear control of a quadrotor micro-UAV using feedback-linearization," in *Proc. IEEE Int. Conf. Mechatronics*, Apr. 2009, pp. 1–6.
[35] B. Wang, D. Zhu, L. Han, H. Gao, Z. Gao, and Y. Zhang, "Adaptive fault-tolerant control of a hybrid canard rotor/wing UAV under transition flight subject to actuator faults and model uncertainties," *IEEE Trans. Aerosp. Electron. Syst.*, early access, Feb. 9, 2023, doi: 10.1109/TAES.2023.3243580.
[36] L. Wang, R. Ortega, H. Su, and Z. Liu, "Stabilization of nonlinear systems nonlinearly depending on fast time-varying parameters: An immersion and invariance approach," *IEEE Trans. Autom. Control*, vol. 60, no. 2, pp. 559–564, Feb. 2015.
[37] K. Xia, W. Chung, and H. Son, "Dynamics estimator based robust fault-tolerant control for VTOL UAVs trajectory tracking," *Mech. Syst. Signal Process.*, vol. 162, Jan. 2022, Art. no. 108062.
[38] J.-J. Xiong and G. Zhang, "Discrete-time sliding mode control for a quadrotor UAV," *Optik*, vol. 127, no. 8, pp. 3718–3722, Apr. 2016.
[39] B. Zhang, X. Sun, S. Liu, and X. Deng, "Adaptive model predictive control with extended state observer for multi-UAV formation flight," *Int. J. Adapt. Control Signal Process.*, vol. 34, no. 10, pp. 1341–1358, Oct. 2020.
[40] Q.-L. Zhou, Y. Zhang, C.-A. Rabbath, and D. Theilliol, "Design of feedback linearization control and reconfigurable control allocation with application to a quadrotor UAV," in *Proc. Conf. Control Fault-Tolerant Syst. (SysTol)*, Oct. 2010, pp. 371–376.

IMIL HAMDA IMRAN received the B.S. degree in electrical engineering from Andalas University, Indonesia, in 2011, the M.S. degree in systems and control engineering from the King Fahd University of Petroleum and Minerals, Saudi Arabia, in 2015, and the Ph.D. degree in electrical engineering from The University of Newcastle, Australia, in 2020.

He was a Post-Doctoral Research Associate with the Department of Engineering, Lancaster University, U.K., in 2022. He is currently a Post-Doctoral Fellow with the Applied Research Center for Metrology, Standards, and Testing, King Fahd University of Petroleum and Minerals. His research interests include networked control systems, multi-agent systems, nonlinear control, and adaptive control.

AZHAR M. MEMON was born in Pakistan, in 1987. He received the B.E. degree in electronics from the National University of Sciences and Technology (NUST), Pakistan, in 2009, the M.Sc. degree in automation and control engineering from the National University of Singapore (NUS), Singapore, in 2010, and the Ph.D. degree from the King Fahd University of Petroleum and Minerals (KFUPM), Saudi Arabia, in 2015.

From 2009 to 2010, he was a Research Engineer with NUS and a Lecturer in 2011. He joined the Research and Development Department, Rosen Group, as a Sensors and Algorithm Specialist. In 2019, he joined KFUPM as an Assistant Professor, where he is actively participating in managing various client-funded and internally funded research projects and teaching. He has authored or coauthored several peer-reviewed research articles and conference papers in reputable journals and international conferences. His research interests include control systems, signal processing, data analytics, nondestructive testing, and aquaponics. Website: www.azharmemon.com.

DILEK FUNDA KURTULUS received the B.S. and M.S. degrees in aerospace engineering from Middle East Technical University, Ankara, Turkey, in 2000 and 2002, respectively, and the Ph.D. degree in aerospace engineering from ENSMA/Université de Poitiers, Poitiers, France.

In 2006, she was Post-Doctoral Researcher with Laboratoire d'Etudes Aérodynamique, ENSMA Poitiers, and Laboratoire de Combustion et Systèmes Réactifs, CNRS, Orléans, France. Since 2018, she has been a Professor with the Department of Aerospace Engineering, Middle East Technical University. Her research interests include aircraft design, unsteady aerodynamics, and unmanned air vehicles.

Dr. Kurtulus was a recipient of the Amelia Earhart Fellow at Zonta International, in 2005, the NATO Scientific Achievement Award, in 2011, the Turkish Academy of Science Young Scientific Award, in 2012, and the Zonta International Centennial Recognition Award of Turkey, in 2019.

SRIKANTH GOLI was born in Hyderabad, India. He received the B.Tech. degree in aeronautical engineering from Jawaharlal Nehru Technological University, in 2008, the M.E. degree in aeronautical engineering from the Hindustan Institute of Technology and Science, in 2011, and the Ph.D. degree from the Department of Aerospace Engineering, IIT Kharagpur, India, in 2019.

From 2019 to 2022, he carried out research at various academic institutions and industries. He is currently a Post-Doctoral Researcher with the Applied Research Center for Metrology, Standards, and Testing (ARC-MST), King Fahd University of Petroleum and Minerals (KFUPM), Saudi Arabia. His research interests include aircraft design, experimental and numerical fluid dynamics, and unmanned air vehicles.

Dr. Goli has memberships in professional societies, such as the National Society of Fluid Mechanics and Fluid Power, the Indian Society of Theoretical and Applied Mechanics, and the Aeronautical Society of India.

LUAI MUHAMMAD ALHEMS received the Ph.D. degree from Texas A&M University, College Station, TX, USA, in 2002. He is currently a Professor of thermo-fluid with the Department of Mechanical Engineering, King Fahd University of Petroleum and Minerals (KFUPM), Dhahran, Saudi Arabia. He is also the Director of the Applied Research Center for Metrology, Standards, and Testing (ARC-MST) Research Institute. Regional authorities have recognized him for his research work. He has authored or coauthored more than 180 journal articles and patents. His research interests include gas turbines, energy systems, failure analysis, wind energy, and energy conservation.